# Dewetting
# PHYS 563 term paper

Chong Han

May 8, 2017

**Abstract**

A substrate that is covered by a film of liquid could dewet if system parameters change. Depending on the surface and liquid, dewetting could result in different patterns. The formation of dry patches starts with nucleation which could be caused by thermal noise, defects or spontaneous capillary waves. The conditions for each pattern has been examined and experimental results confirm theoretical predictions. The dynamics of hole formation is also studied and compared to hydrodynamics theory.

# 1   Introduction

Wetting is the ability of a liquid to maintain contact with a solid surface. When a liquid is deposited on the surface of a solid, liquid will spread out in some cases and this process is called spreading. Dewetting, on the contrary, is the inverse process. A thin liquid film is present on a solid substrate and when the liquid is not stable it could bead up and form dry patches. Understanding the dewetting process and the conditions of dewetting are of technological importance. In some cases (e.g. coating and dielectric layers) we want to maintain the film and avoid dewetting while in other cases (e.g. windscreens) we want to speed up the dewetting process.

In this paper, we first examine some basic theory in wetting and spreading since wetting and dewetting are closely related. Then the effective interface potential is introduced and three types of dewetting patterns are discussed. It is shown experimentally and theoretically how the effective potential affect the dewetting pattern. The experiment fits well with the theory and an effective interface potential could be reconstructed by measuring the dewetting process. Another experiment on the dynamics of the dewetting is also shown in this paper. The dewetting speed is found to be a constant in time.

# 2   Basis of wetting

To understand the process of dewetting, some basic theory of wetting should be looked at first. Considering a liquid drop on a solid substrate, there are three different phases in the system: the liquid, the solid and the vapor. At equilibrium, if we consider the force balance at the three-phase contact line, the following equation can be obtained easily from Fig. 1[1]

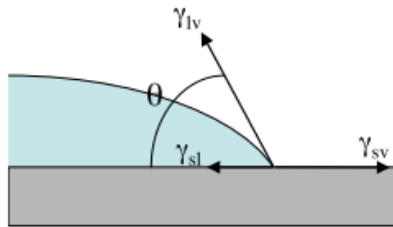$$\gamma_{SV} = \gamma_{SL} + \gamma_{LV}\cos\theta_e, \tag{1}$$



Figure 1: Diagram for Equation 1. The surface tension is equivalent to force per unit length at the contact line

where $\gamma_{SV}, \gamma_{SL}, \gamma_{LV}$ are solid-vapor, solid-liquid and liquid-vapor surface tension respectively. $\theta_e$ is the equilibrium contact angle. If surface tensions on each surfaces are known, the equilibrium angle can be easily calculated. To further distinguish different wetting state, the equilibrium spreading coefficient is defined as [1]

$$S_{eq} = \gamma_{SV} - (\gamma_{SL} + \gamma_{LV}) = \gamma_{LV}(\cos\theta_e - 1). \tag{2}$$

This coefficient is defined so that $S_{eq} \leq 0$ and the system is completely wet when $S_{eq} = 0$. There is also a case where $\theta_{eq} = \pi$ which is completely dry. This case is rare in practice (except mercury on glass). For solid substrate, the difference $\gamma_{SV} - \gamma_{SL}$ is a property of the solid and independent of the liquid used. So the contact line angle can be determined if the surface tension of liquid-surface is known and the difference is known for the solid.
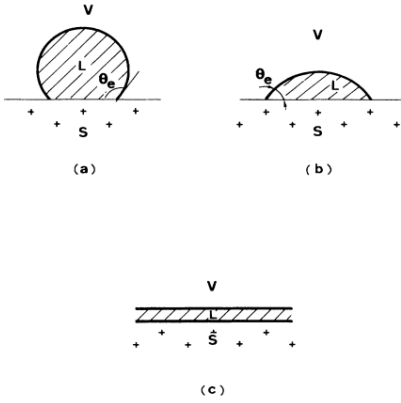


Figure 2: (a) and (b) correspond to partial wetting where $S_{eq} < 0$. $S_{eq\,a} < S_{eq\,b}$ (c) corresponds to $S_{eq} = 0$.

However, in most cases, the system is not in equilibrium. When the liquid is deposited on the surface initially, it may take a long time for the system to reach equilibrium. To determine whether the liquid would spread or not, the initial spreading coefficient is defined as

$$S_i = \gamma_{S0} - (\gamma_{SL} + \gamma_{LV}), \tag{3}$$

Here $\gamma_{S0}$ is the surface tension of dry solid substrate. Following the Gibbs absorption equation [2], $\gamma_{S0} > gamma_{SV}$ and $S_i > S_{eq}$. Generally $\gamma_{S0}$ and $\gamma_{SV}$ could differ a lot, making $S_i$ large and positive and difficult to determine $S_{eq}$ from surface tension of pure substances.

# 3  Intermolecular forces

The effect of intermolecular forces on wetting can be quantified by considering a liquid film of thickness $l$ on a solid substrate. If the solid-liquid adhesive interactions is strong, the system can lower the total energy by increasing $l$, resulting a pressure between the solid-liquid and the liquid-vapor interfaces. This pressure is called disjointing pressure and can be derived from effective interface potential $V(l)$,

$$\Pi(l) = -dV(l)/dl. \tag{4}$$

Using Lennard-Jones potential

$$V = \epsilon[(r_m/r)^{12} - 2(r_m/r)^6], \tag{5}$$

the attractive long-range van der Waals force can be described by the $r^{-6}$ term. Performing a volume integral over the two half spaces bounding the film, the disjointing pressure can be calculated to be $\Pi(l) = A/6\pi l^3$. Here $A$ is called Hamaker constant. Integrating $\Pi(l)$ using 4, the effective interaction energy is estimated to be

$$V(l) = \frac{A}{12\pi l^2}. \tag{6}$$

The Hamaker constant is a key property for determining the wetting behaviour[1]. For partial wetting, $S_{eq} < 0$; the sign of $A$ does not matter in this case. When $S_{eq} = 0$ and $A > 0$, a wetting layer would form and corresponds to complete wetting. When $S_{eq} \approx 0$ and $A < 0$, a mesoscopic wetting film would form and this is called frustrated complete wetting.

# 4  Dewetting

To measure the behaviour of dewetting, a uniform liquid layer is placed on a solid that is not wettable. Unless the film is thick enough that could be stabilized by gravity, the film would become unstable and dry spots would form. The initial formation of dry patches are categorized into three groups due to different formation of holes. If the system is perturbed by defects or dust particles, it is called heterogeneous nucleation. The nucleation could also be driven by thermal noise which is called thermal nucleation (or homogenous nucleation). The last mechanism is caused by spontaneously amplified capillary waves which is known as spinodal wetting.

It is shown that spinodal wetting is possible only if the second derivative of $V$ with respect to film thickness is negative, $V''(h_0) < 0$[3] . Figure 3 shows three typical form of interface potential $V$. Curve (1) is a curve that global minimum is at infinite thickness. This curve represents a stable film as the $V''(h) > 0$

and the thickness of the film tends to grow to infinity. Curve (2) is a curve with global minimum at $h = h^*$. If the initial thickness $h_0$ is larger than $h^*$, $V''(h_0) < 0$ and the film will dewet. After dewetting, the solid is not completely dry. Instead, a layer with thickness $h^*$ will be left on the substrate. Curve (3) represents a metastable film. The film is unstable at small film thickness but could be stable at larger thickness.
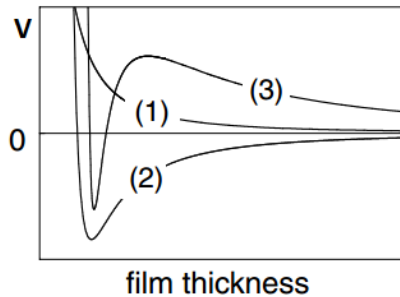


Figure 3: Sketch of interface potential as a function of film thickness for (1) stable, (2) unstable and (3) metastable

In the case of spinodal dewetting, although all fluctuations in film thickness are amplified, there is a preferred wavelength $\lambda_s$ that is connected to $V''(h)$ by

$$\lambda_s(h) = \sqrt{\frac{-8\pi^2 \gamma_{LV}}{V''(h)}}. \tag{7}$$

This preferred wavelength could be measured by a Fourier transform as shown latter in the next section.

## 4.1 Experiments on dewetting of polystyrene and reconstruction of interface potential

An experiment done in [3] showed these three different dewetting patterns and managed to reconstruct the interface potential. Solid substrate in this experiment is silicone with a silicone oxide layer with different thickness. Then a liquid layer of polystyrene is deposited onto the substrate the dewetting process is monitored. The thickness of the silicon oxide layer are 1.7nm, 2.4nm and 191nm respectively.
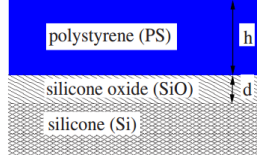
Figure 4: Sketch for the liquid-solid interface

Some results of this experiment is shown in Fig. 5. In (a) to (c), the scale bar length is 5 $\mu m$. (a) is 3.9 nm liquid on 191nm silicon oxide layer. (b) is 4.1nm liquid on 2.4nm SiO layer and (c) is 6.6nm liquid on 2.4nm SiO. Changing the thickness of the SiO layer would effectively change the interface potential and changing the thickness of liquid layer would move the position on the potential curve. Thus all three dewetting patterns can be observed in this one system. $\lambda_s$ can be obtained by doing a Fourier transform on the image such as (a).
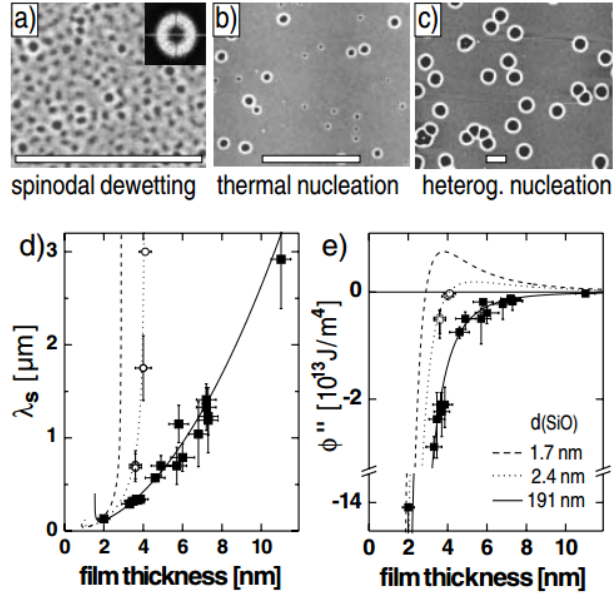


Figure 5: (a)-(c) Three types of dewetting patterns. (d) $\lambda_s$ versus $h$ (e) $V''(h)$ versus h

Making different thickness of liquid layer and repeat the experiment, the $\lambda_s$ can be plotted as in (d). The filled squares are on 191 nm SiO and open circles are on 2.4nm SiO. For 2.4nm SiO, liquid thicker than 4.1nm lead to heterogenous nucleation shown in (c) instead. Using Equation 7, the $V''(h)$ could be

calculated and the results are shown in (e).

p Now using Equation 6, the data from Fig. 5(e) can be fitted and the $A$ can be extracted from the fit. For 191nm SiO, the effect of Si can be ignored and the Hamaker constant $A$ is simply $A_{SiO}$. To make the interface potential have a global minimum, besides van der waals potential in Equation 6, another short-range term is also included for further fitting. Then for smaller SiO thickness, the effect of Si should also be considered. After all the fitting, the final effective potential for three thickness are plotted in Fig. 6. We can see that in Fig. 5(a), the spinodal nucleation happens in the region that $V''(h) < 0$. The thermal nucleation in Fig. 5(b )happens near $V''(h) = 0$ and the heterogenous nucleation in Fig. 5(c) happens at $V''(h) > 0$.
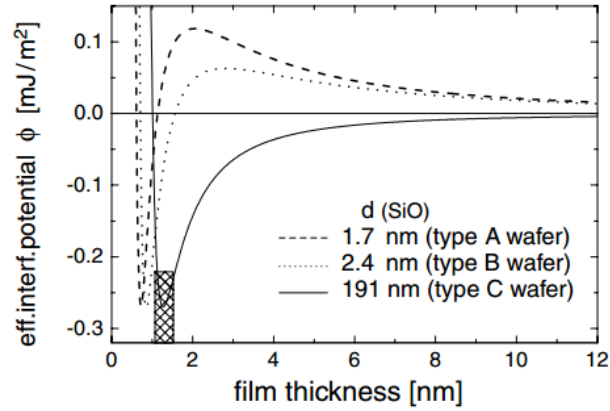


Figure 6: Reconstructed effective interface potential on 3 different thickness of SiO

This experiment showed that the wettability of the Si/SiO layer can be tuned by the thickness of the SiO layer and the experiments can be explained well by the effective interface potential. All three types of dewetting patterns are observed and they are theoretically expected.

## 4.2 Dynamics of dewetting

In nucleation regime, the growth of individual hole is examined in [5]. In their paper, a hole is created initially and the evolution of the film is monitored by a video camera. The hole is circular at most times besides a few defects around the contact line. The liquid removed from the dry hole forms a rim around the hole shown in Fig. 7. The radius of the circle could be easily obtained from the images and the dynamic contact angle is obtained using a optical reflectivity method.

As the result of the experiment, the receding velocity is observed to be lin-
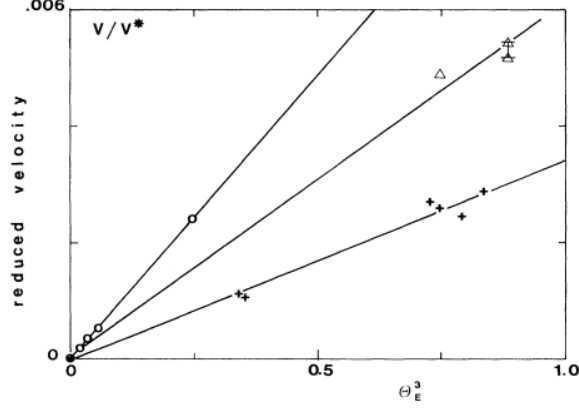
Figure 7: Reduced velocity versus equilibrium contact angle $\theta_e$. Different lines are for different liquids in this plot

ear throughout the experiment. The dynamic contact angle $\theta_d$ is smaller than equilibrium contact angle $\theta_e$ and shows a fixed ratio

$$\theta_d/\theta_e = 0.7 \pm 0.2. \tag{8}$$

The viscosity of the liquid used also played a role in receding velocity and it is found to be a simple inverse relation. Thus we can define a reduced velocity $V/V^*$ where $V^* = \gamma_{LV}/\eta$ which should be constant when only viscosity $\eta$ is changed. When changing the solid substrate surface, the reduced velocity showed a linear relationship with $\theta_e^3$ as shown in Fig. 7,

$$V/V^* = k\theta_e^3. \tag{9}$$

Following procedures in [6], we can get the following equations.

$$\frac{1}{2}\gamma(\theta_e^2 - \theta_d^2) = 3\eta L\theta_d^{-1}V_A, \tag{10}$$

$$\frac{1}{2}\gamma\theta_d^2 = 3\eta L\theta_d^{-1}V_A. \tag{11}$$

The left-handed sides are Young forces and they should be compensated by the viscous force due to the flow. The $V_A$ and $V_B$ are inner and outer velocity of the rim. In this experiment the $V_A$ and $V_B$ are basically same, resulting the following equations,

$$\theta_d = \theta_e/sqrt2 \tag{12}$$

$$V/V^* = (1/12L\sqrt{2})\theta_e^3. \tag{13}$$

These theoretical predictions are confirmed by the experiments result Equation8,9.

8

# 5 Conclusion

This paper discussed some basic theory of wetting and dewetting and showed a few experiments on the dewetting process. The wetting and spreading process are relatively well-understood but little work is done on this reverse process. Using the Hamaker constant and reconstructing interface potential energy, the wetting ability of the substrate can be controlled by tuning the thickness of the layer. The Dewetting spread velocity is also measured and its relationship with viscosity and surface are calculated. The measurement fits well with the theoretical expectation. However, the liquid used in experiments shown in this paper is made of polymers, which is non-Newtonian fluid. Some of the behaviour may need additional parameters such as viscoelasticity to explain. There are also many works recently studying the shape of the profile near the dewetting front which is not discussed in this paper.

# References

[1] Bonn, D., Eggers, J., Indekeu, J. and Meunier, J. (2009). *Wetting and spreading.* Reviews of Modern Physics, 81(2), 739-805.

[2] Rowlinson, J. S., and B. Widom, 1982, *Molecular Theory of Capillarity* (Clarendon, Oxford).

[3] Seemann, R., S. Herminghaus, and K. Jacobs, 2001, *Dewetting patterns and molecular forces: A reconciliation,* Phys. Rev. Lett. 86, 5534.

[4] Seemann, R., S. Herminghaus, and K. Jacobs, 2001, *Gaining control of pattern formation of dewetting liquid films,* J. Phys.: Condens. Matter 13, 4925.

[5] Redon, C., F. Brochard-Wyart, and F. Rondolez, 1991, *Dynamics of dewetting,* Phys. Rev. Lett. 66, 715.

[6] de Gennes, P.-G., 1985, *Wetting: statics and dynamics,* Rev. Mod. Phys. 57, 827.